

# Design of Green Engineered Cementitious Composites for Improved Sustainability

by Michael D. Lepech, Victor C. Li, Richard E. Robertson, and Gregory A. Keoleian

*The sustainability of the built environment is increasingly coming to the forefront of infrastructure design and maintenance decisions. To address this, development of a new class of more sustainable cement-based materials is needed. These materials should be developed with respect to the final application in which they will be used. Neglecting the connection between material development, structural design, and sustainability objectives can lead to shorter-lived, costly, and resource-intensive structures that require greater maintenance. Within this study, a green materials design framework is presented and used to complete a case study in the design of green materials for a specific infrastructure application. Through deliberate control of composite constituents and the interactions among them, cement-based composites have been developed that incorporate industrial waste streams while not sacrificing critical material properties.*

**Keywords:** engineered cementitious composite (ECC); green chemistry; green materials; sustainability; sustainable infrastructure.

## INTRODUCTION AND CURRENT CONCRETE PRACTICE

Sustainability initiatives can be traced back to the environmental movement of the 1960s and the energy crisis of the 1970s. Globally, there are a number of academic, industrial, and government initiatives actively improving the sustainability of built environments.<sup>1-3</sup> These efforts focus on green materials development and procurement, design for low-energy demand, and construction methods that produce less waste, use fewer resources, and require less energy.

One approach to reducing the environmental impact (that is, “greening”) of concrete has been the use of fly ash and blast-furnace slag as supplementary cementitious materials (SCMs). A by-product of coal-fired power generation and used since the mid-1970s, fly ash replaces cement while increasing workability through improved particle gradations and decreasing environmental impacts by reducing land-filling and replacing energy-intensive cement.<sup>4,5</sup> Improvements in the durability of concrete have also been found.<sup>6-8</sup> This has been attributed to the densified matrix and accompanying lower transport.<sup>9</sup> Recently, Wang and Li<sup>10</sup> successfully used high volumes of fly ash in strain-hardening cementitious materials.

Blast-furnace slag, a pozzolanic by-product of steel blast furnaces, can also be used as a cement substitute for lowering environmental impact.<sup>11</sup> Benefits from using fly ash or ground-granulated blast-furnace slag include reductions in energy consumption, greenhouse gas releases, and other pollutant emissions from initial mining of limestone, calcination, and grinding.<sup>12</sup> Successful industry acceptance of both fly ash and blast-furnace slag is noted by respective ASTM standards (ASTM C618 and ASTM C989).

Recycled aggregates and industrial wastes have also been introduced as alternatives with lower environmental impacts. In many developed countries, the availability of high-quality

aggregates is decreasing. By reclaiming aggregates, the supply can be extended. Unlike fly ash and blast-furnace slag, however, recycled aggregate concretes have met resistance, particularly by departments of transportation concerned with lower strength and durability.<sup>13</sup> Nontraditional waste streams have also been explored to reduce impact. These include shredded waste automobile tires,<sup>14</sup> municipal solid waste ash,<sup>15,16</sup> rice husk ash,<sup>17</sup> ground waste glass,<sup>18,19</sup> and reclaimed harbor dredging waste.<sup>19</sup>

While industrial wastes can reduce the environmental impact of concrete per volume, this is not a sufficient indicator of overall sustainability. Effects of material changes on the larger system must be considered. Keoleian et al.<sup>20</sup> found that due to the long service life of concrete infrastructure, the influence of material durability on the overall sustainability (economic, environmental, and social) is large. If incorporating industrial wastes lowers durability, more frequent maintenance, repair, and replacement of infrastructure are required. Keoleian et al. found that bridges incorporating conventional materials with lower initial environmental impact but poorer durability consumed greater volumes of material throughout their total life cycle. This greater consumption ultimately lowered the sustainability of these systems while using materials originally thought to be more sustainable.

## New approach: engineered cementitious composites

Material durability plays a central role in sustainable concrete infrastructure. Therefore, adverse effects of industrial waste on durability should be controlled. Engineered cementitious composite (ECC) was identified as a candidate for material greening with the overall goal of improving sustainability. ECC is a high-performance fiber-reinforced cementitious composite (HPFRCC) designed to resist large tensile and shear forces while remaining compatible with ordinary concrete in almost all other respects such as compressive strength and thermal properties.<sup>21</sup> As noted by Lepech and Li,<sup>22</sup> ECC materials are highly durable in a number of harsh environments. This durability results from unique pseudo strain-hardening ductility and distributed microcracking behavior in tension.

To achieve tensile ductility and distributed microcracking, ECC is designed using a well-defined toolbox of micro-mechanical models. These models characterize crack formation and fiber bridging within the loaded composite.<sup>23,24</sup> The tensile response and microcracking behavior of ECC are

*ACI Materials Journal*, V. 105, No. 6, November-December 2008.

MS No. M-2007-388 received November 21, 2007, and reviewed under Institute publication policies. Copyright © 2008, American Concrete Institute. All rights reserved, including the making of copies unless permission is obtained from the copyright proprietors. Pertinent discussion including authors' closure, if any, will be published in the September-October 2009 *ACI Materials Journal* if the discussion is received by June 1, 2009.

**Michael D. Lepech** is a Research Fellow at the University of Michigan's Center for Sustainable Systems. He received his BSE, MSE, and PhD in Civil Engineering from the University of Michigan, Ann Arbor, MI. His research interests include the development of durable high-performance cementitious composites and the design of sustainable infrastructure systems.

ACI member **Victor C. Li** is a Professor of Civil and Environmental Engineering and Material Science and Engineering at the University of Michigan. He is a member of ACI Committee 544, Fiber Reinforced Concrete. His research interests include micromechanics-based composite materials design and engineering, innovative structures design based on advanced materials technology, and sustainable infrastructure engineering.

**Richard E. Robertson** is a Professor of Material Science and Engineering at the University of Michigan. His research interests include molecular dynamics of mechanical relaxation of polymers to the high-speed, low-cost manufacturing of fiber composite structures, including the fracture process in polymers and composites and failure analysis.

**Gregory A. Keoleian** is a Professor in the School of Natural Resources and Environment at the University of Michigan. His research interests include the development of life cycle assessment tools for quantifying and characterizing the environmental burdens associated with a product or system life cycle.

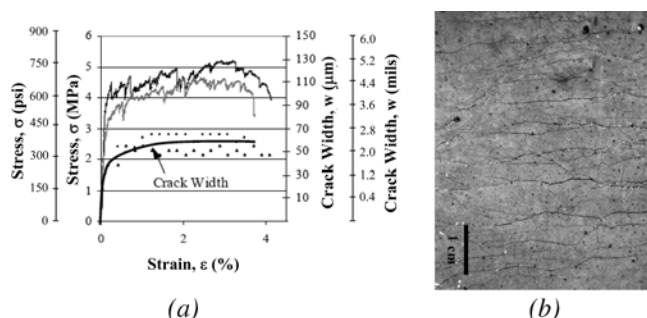


Fig. 1—Composite response in uniaxial tension for ECC material: (a) stress-strain and crack width development characterization; and (b) microcracking behavior.

shown (Fig. 1 with mixture design in Table 1). Key to this response are microcracks that widen to 60  $\mu$  (0.002 in.) at 1% tensile strain, and remain at this width as deformation increases (Fig. 1(a)). During this process, further deformation is accommodated by additional microcracks saturating the ECC (Fig. 1(b)) before localization. This tight crack width is essential to durability because preloaded ECC continues to exhibit water permeability equal to sound ECC or concrete even at 3% deformation.<sup>25</sup>

The objective of this work is the development of a new framework for green infrastructure materials design. By validating this framework, low-environmental-impact material substitutes are identified, and a new version of green ECC that incorporates a number of industrial wastes is designed for use in bridge infrastructure.

## RESEARCH SIGNIFICANCE

Concrete is the most used anthropogenic material worldwide.<sup>26</sup> The enormous concrete material flows cause significant societal and environmental impacts.<sup>26</sup> Cement production accounts for 5% of global greenhouse gases<sup>27,28</sup> and significant levels of NO<sub>x</sub>, particulates, and other pollutants.<sup>29-31</sup> Developing countries require infrastructure expansion; however, the unsustainable interaction between built and natural environments is increasingly a global concern. The establishment of a framework for systematic screening and design of materials, which reduces environmental impact through the introduction of low-impact material streams while maintaining high material performance, provides a foundation for more sustainable infrastructure design.

**Table 1—Mixture proportions and fresh flowability results for ECC material (mixture designation M45) along with green ECC mixture proportions (ECC with green foundry sand, ECC with bag house calcinator sand)**

Mixture proportions, *high-range water reducer	M45	M45G	M45 Calcin
Cement	1	1	1
F-110 sand	0.8	—	—
Green sand	—	0.8	—
Calcinator sand	—	—	0.8
Fly ash	1.2	1.2	1.2
Water	0.58	0.57	0.58
*High-range water reducer	0.013	0.03	0.013
PVA fiber	0.02	0.02	0.02
<b>Fresh properties</b>			
Average diameter, mm (in.)	885 (34.8) $\pm$ 73 (2.9)	915 (36.0) $\pm$ 87 (3.4)	960 (37.8) $\pm$ 63 (2.5)
$\Gamma$	3.4 $\pm$ 0.4	3.6 $\pm$ 0.4	3.8 $\pm$ 0.3
<b>Material sustainability indexes</b>			
Solid waste, kg/L	−0.49	−0.96	−0.96
Carbon dioxide, kg/L	662.7	660.8	660.8
PM <sub>10</sub> , g/L	5.8 $\times$ 10 <sup>−4</sup>	4.0 $\times$ 10 <sup>−6</sup>	4.0 $\times$ 10 <sup>−6</sup>
Primary energy, MJ/L	6.64	6.63	6.63

## MATERIAL DESIGN METHODOLOGY

### Material design framework and preliminary screening and assessment

The development process for green ECC comprises a number of stages (Fig. 2). This process is part of a larger sustainable concrete infrastructure paradigm proposed by Keoleian et. al.<sup>32</sup> This paradigm (Fig. 3) integrates materials design with infrastructure service life evaluation and life cycle analysis. Specifically, Fig. 2 details the “Input Materials and Composition,” “Microstructure Tailoring,” “Material Physical Properties,” and “Infrastructure Application” portions of Fig. 3. The iterative design of materials, evaluation of structural performance, assessment of life cycle impacts, and the redesign of materials provides for integration between engineering and life cycle analyses.

To begin material design, a pool of candidate substitute materials is gathered with no potential materials excluded. While industrial wastes have high potential due to low cost and large material flows, any material with comparatively low environmental impacts, including recycled cementitious materials or aggregate, can be evaluated. Development begins with preliminary screening designed to limit the number of substitutes, which undergo rigorous investigation.

Preliminary screening focuses on three factors: mechanical properties, chemical properties, and material environmental sustainability. Mechanical properties may include the strength or stiffness of various substitutes. Preliminary chemical analysis evaluates adverse chemical interactions that replacements may have with other constituents or the intended application environment (that is, the presence of chlorides or corrosives). Environmental sustainability is evaluated through material sustainability indexes (MSI). MSI values capture environmental indicators such as global warming potential, water used, or energy intensity in material production, without regard for the application, and allow for comparison of green materials on a per volume basis. These are calculated using life cycle assessment techniques that provide a comprehensive accounting for all energy and

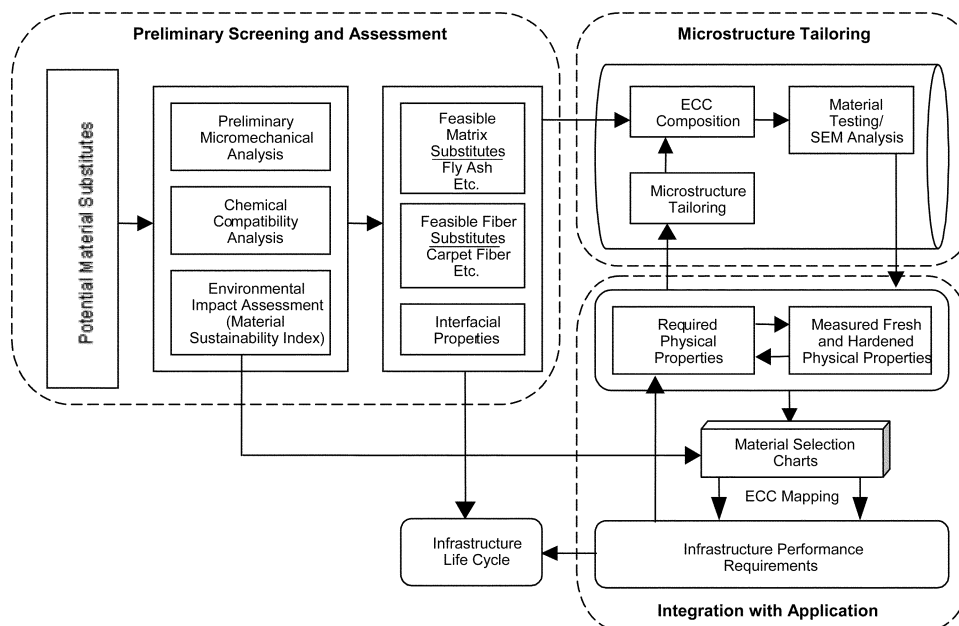


Fig. 2—Schematic of green ECC materials development framework.

material inputs, along with emissions and wastes generated during material production including raw material extraction and processing.<sup>33</sup> Typical MSI values are shown in Table 1.

A large pool of substitutions is initially considered. For ECC, potential substitutes were grouped into three main groups: binder (cement), filler (sand), and fiber. For each group, mechanical, chemical, and environmental preliminary screening was conducted (left portion of Fig. 2). Preliminary screening parameters for cement replacements included grain size distributions, hydration potential, material flow estimation, and MSI evaluation. Parameters for sand replacements included adverse chemical effects (that is, alkali-silica reaction and chlorides), grain size distribution, material flow estimation, and MSI evaluation. Screening parameters for fiber replacements included fiber strength, modulus, maximum elongation, diameter, length, material flow estimation, and MSI evaluation. Parameters were derived from theoretical limits based on micromechanical tailoring (that is, grain size distribution and fiber strength)<sup>34</sup> or practical limits of processing or procurement (that is, fiber length and material availability).

Reductions in MSI values captured the lower environmental impacts of the entire composite (per L) by incorporating wastes or using low-impact virgin substitutes. Building from a life cycle inventory of ECC constituents,<sup>32,33</sup> MSI values could include primary energy consumption (MJ/L), carbon dioxide equivalent release (equivalent grams of CO<sub>2</sub>/L), PM<sub>10</sub> release (grams of PM<sub>10</sub>/L), biological oxygen demand (grams of BOD/L), along with solid waste generated (kg/L) (Table 1). While most ECC environmental impacts stem from cement production, MSI values can be used as a preliminary guide to material greening by eliminating substitute wastes with large environmental impact (due to excessive processing or toxicity) from being considered.

### Material mapping and integration with application

As discussed, durability is an important element in materials design for sustainable infrastructure. Design for durability is closely linked with an understanding of specific structural

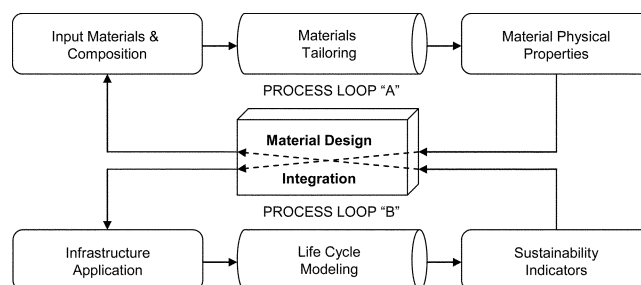


Fig. 3—Interactive design framework for sustainable infrastructure systems.

demands and associated material requirements. This linking of material design with a specific infrastructure application (lower right portion of Fig. 2) was made up of three distinct steps. First, independent of materials development, an infrastructure application was targeted, and sources of failure with existing technologies were identified. These sources were application-specific, and could range from steel corrosion caused by leaking bridge joints to fatigue failure and reflective cracking in rigid pavement overlays.

Second, these performance requirements were linked through structural modeling to required material properties. In the case of bridge joints, these could be replaced by ductile “link slabs,” which replace joints with a strip of ECC, allowing for thermal expansion and contraction of bridge spans while creating a continuous, impermeable deck.<sup>35</sup> Within the link slab, ECC tensile ductility coupled with tight crack widths were the most critical elements to structural durability. In this regard, ECC materials were not intended to be a replacement for all concrete infrastructure materials. Rather, ECC was intended for strategic application within concrete infrastructure in circumstances where the brittle behavior of concrete specifically limited structural, durability, or environmental performance (that is, replacement of expansion joints).

Third, the required material properties were compared with actual physical properties (that is, tensile ductility,

**Table 2—Potential substitute materials and preliminary evaluation results**

Material	Substituting material	Outcome	Reason
Fly ash	Cement	Passed	—
Cement kiln dust	Cement	Passed	—
Granulated blast-furnace slag	Cement	Failed	Poor grain size distribution
Rice husk ash	Cement	Failed	Poor hydration
Solid municipal waste ash	Cement	Failed	Inconsistent chemistry
Foundry green sand	Sand	Passed	—
Waste water sludge	Sand	Failed	Inconsistent chemistry
Expanded polystyrene beads	Sand	Passed	Micromechanical synergy
Pot lining	Sand	Failed	Chemical incompatibility
Post-consumer carpet fiber	Fiber	Passed	Micromechanical synergy
Banana fiber	Fiber	Failed	Low strength

maximum crack widths and tensile strength) of the new material. If actual properties did not meet requirements, the material was re-engineered using the micromechanical tools described in the following. This tight linking of material with structural design and application offered a high degree of efficiency in material consumption and energy use by maximizing industrial waste contents while not sacrificing overall structural performance.

### Materials tailoring—grain size distribution

Building from the pool of screened substitutes and using material goals set by the final application, the iterative materials tailoring process began (upper right portion of Fig. 2). Grain size distribution of sand substitutes was critical to meet ECC workability requirements. In addition to restricting maximum particle size, Fischer et al.<sup>36</sup> and Lepech and Li<sup>37</sup> proposed a set of ECC design procedures for processing. Grain size distributions of the various ECC components were designed to produce a free-flowing mixture during mixing, and a self-consolidating material during casting. Relying on control of combined grain-size distributions to achieve a highly dense and closely packed matrix, this approach was analogous to densely packed soils that were subject to liquefaction in earthquakes. In particular, the Alfred grain size distribution curve was proven successful (Eq. (1))<sup>38</sup>

$$f_d = 100 \left( \frac{D^q - D_s^q}{D_L^q - D_s^q} \right) \quad (1)$$

where  $f_d$  is the cumulative percent of particles finer than  $D$ ;  $D$  is the size of any particle, in mm;  $D_s$  is the diameter of smallest particle in distribution, in mm;  $D_L$  is the diameter of largest particle in distribution, in mm; and  $q$  is the distribution modulus.

To quantify the effects of particle size distribution, a flowability testing follows procedures outlined by Kong et al.<sup>39</sup> A standard concrete slump cone is filled with fresh ECC and discharged onto a level Plexiglas or glass plate. Following discharge, two orthogonal diameters of the ECC “pancake” are averaged, and a characteristic flowability factor, denoted by  $\Gamma$ , is calculated using Eq. (2)

$$\Gamma = \frac{(D_1 - D_0)}{D_0} \quad (2)$$

where  $\Gamma$  is the fresh ECC deformability factor;  $D_1$  is the average of two orthogonal “pancake” diameters, in mm; and  $D_0$  is the diameter of bottom of original slump cone, in mm.

### Materials tailoring—micromechanics

Ductility is the cornerstone of ECC mechanisms that improve structural durability. The fundamental micromechanics that govern this ductile behavior through the formation of multiple microcracks provide an additional tool for composite design. The basis of multiple cracking and strain hardening within ECC is the propagation of steady-state cracks, first characterized by Marshall and Cox<sup>40</sup> for continuous aligned fiber-reinforced ceramics, and extended to fiber-reinforced cementitious composites by Li and Leung<sup>41</sup> and Lin et al.<sup>42</sup> The formation of multiple steady-state cracks is governed by the bridging stress versus crack width opening relation and fracture toughness of the mortar matrix. To achieve strain hardening, the inequality shown in Eq. (3) must be satisfied

$$J'_b = \sigma_0 \delta_0 - \int_0^{\delta_0} \sigma(\delta) d\delta \geq J_{tip} \approx \frac{K_m^2}{E_m} \quad (3)$$

where  $J'_b$  is the complimentary energy;  $\sigma_0$  and  $\delta_0$  are the maximum crack bridging stress and corresponding crack opening, respectively;  $J_{tip}$  is the fracture energy of the mortar matrix crack tip;  $K_m$  is the fracture toughness of the mortar matrix; and  $E_m$  is the elastic modulus of the mortar matrix.

In addition to this energy criterion, a strength criterion (Eq. (4)) must be satisfied

$$\sigma_0 > \sigma_{cs} \quad (4)$$

where  $\sigma_0$  is the maximum crack bridging stress, and  $\sigma_{cs}$  is the cracking strength of the mortar.

Both  $\sigma_0$  and  $\sigma_{cs}$  may vary from one crack plane to another. For saturated multiple cracking, Li et al.<sup>34</sup> found that Eq. (4) must be satisfied when a crack initiates at  $\sigma_{cs}$ , and  $\sigma_{cs}$  must be below the values of  $\sigma_0$  of each the existing multiple cracks.

## LABORATORY INVESTIGATION

### Preliminary assessment results

The results of the preliminary screening are shown in Table 2. Both fly ash and cement kiln dust passed as cement replacements for further micromechanical analysis and tailoring. This is due to favorable grain size distributions (Fig. 4), good hydration potential, large material flows, and favorable MSI values. Granulated blast-furnace slag was rejected due to large particle size (greater than 300  $\mu$  [0.012 in.]) and high particle porosity that significantly increases water requirements. While Kim et al.<sup>43</sup> demonstrated that ground-granulated blast-furnace slag, with an average particle diameter of 11  $\mu$  (0.0004 in.), can be used within green ECC and produce uniaxial tension strain capacities over 2.5%, this investigation excluded materials that require further processing and additional energy. Slag particles produced directly from the blast furnace are over 300  $\mu$  (0.012 in.) in

average diameter. The use of energy-intensive processes, such as grinding, to refine the waste stream deteriorates composite MSI values.

Rice husk ash and solid municipal waste ash were rejected due to chemical incompatibilities. While the chemical composition of the rice husk ash tested met requirements for ASTM C618 chemical composition of  $\text{SiO}_2$ ,  $\text{Al}_2\text{O}_3$ , and  $\text{Fe}_2\text{O}_3$ , the water requirement (ASTM C618) was nearly 110% and resulted in poor fiber dispersion and fresh properties. Solid municipal waste ash was eliminated due to a high chemical variability. Additionally, Mangialardi et al.<sup>16</sup> found that the levels of combined  $\text{SiO}_2$ ,  $\text{Al}_2\text{O}_3$ , and  $\text{Fe}_2\text{O}_3$  within most municipal solid waste fail to meet required limits within ASTM C618 without additional processing of the ash. Mangialardi et al. found a propensity for accidental retention of heavy metals from illegal waste disposal. Future leaching of these metals is a concern.

A number of sand replacements were considered, including a variety of waste foundry materials, industrial waste water sludge, pot lining from aluminum casting, and waste-expanded polystyrene (EPS) beads from lost foam metal casting. Three separate waste foundry streams were examined. Preliminary mechanical screening for sand replacements focused on grain size distribution. Building from steady state flat crack theory, the maximum particle size within ECC must be below roughly  $200\ \mu$  ( $0.008\ \text{in.}$ ) to keep the fracture toughness  $J_{\text{tip}}$  of the matrix low, and to prevent large matrix particles from dominating fiber dispersion.<sup>34</sup>

Three separate foundry sand waste streams were examined, which are referred to as “bag house sand from calcinators,” “foundry green sand,” and “corbitz.” Bag house sand from calcinators is captured by foundry dust collection systems. Due to vacuum collection, particle sizes are small and very consistent (Fig. 4), and are nearly identical in appearance and mechanical properties to virgin sand currently used for ECC. Green foundry sand is waste from lost foam metal casting. While the size distribution is larger than virgin sand, the green sand grain size distribution ranging up to  $300\ \mu$  ( $0.012\ \text{in.}$ ) was within range of the  $200\ \mu$  ( $0.008\ \text{in.}$ ) grain size limit to warrant further investigation and, unlike blast-furnace slag, did not exhibit high porosity. Corbitz is a by-product from chemically bonded lost foam sand casting, and often contains cobble-sized pieces. While these can be sieved, the chemically bonded corbitz sand adsorbs a number of hazardous chemicals, including high levels of phenols, trichloroethene, and toluene, which coat the sand after casting.<sup>44</sup> As with municipal solid waste ash, chemical hazards rule out the use of corbitz as a substitute.

Dried wastewater sludge from foundry wastewater treatment was also examined. This material contained many particles larger than  $400\ \mu$  ( $0.016\ \text{in.}$ )—too large for ECC. Expanded polystyrene beads, a by-product from lost foam casting, were also too large for sand replacement, with most on the order of 1 to 2 mm ( $0.04$  to  $0.08\ \text{in.}$ ) in diameter.

Waste fibers were considered as replacements for polyvinyl alcohol (PVA) fibers. Li et al.<sup>34</sup> found that fibers within ECC must have a minimum tensile strength of 1000 MPa (145 ksi), an inelastic failure strain greater than 5%, and a fiber diameter between 30 and  $50\ \mu$  ( $0.001$  and  $0.002\ \text{in.}$ ). Banana fibers and post-consumer carpet fibers (nylon and polypropylene) were considered. All fiber replacements fail to meet minimum values (Table 3). Physical properties for PVA and PE (polyethylene) fibers successfully used in ECC are also shown.

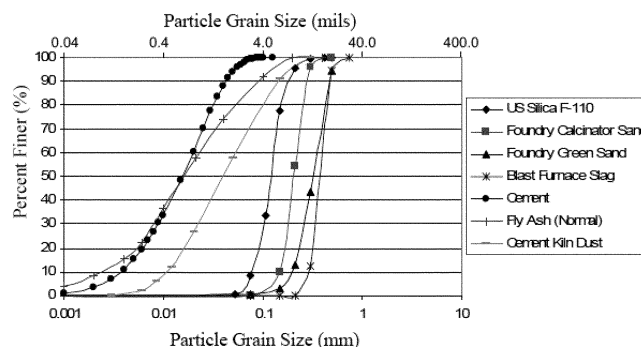


Fig. 4—Virgin and waste material grain size distributions.

**Table 3—Physical properties of current and potential ECC fiber replacements**

Fiber type	Strength, MPa (ksi)	Minimum elongation, %	Diameter, mm (mils)
PVA REC-15 <sup>33</sup>	1620 (235)	6	39 (1.5)
PE <sup>33</sup>	1660 (241)	6	14 (0.55)
Nylon <sup>50</sup>	100 to 750 (14.5 to 109)	10 to 35	50 (2.0)
PP <sup>49</sup>	200 to 600 (29 to 87)	20+	120 to 250 (4.7 to 9.8)
Banana <sup>50</sup>	700 to 800 (102 to 116)	1 to 2	15 to 30 (0.59 to 1.2)

Overall, a small number of green substitutes passed preliminary screening (Table 2). This, however, does not exclude failed substitutes from further examination. Recently, Wang and Li<sup>45</sup> found that artificial flaws embedded within the mortar matrix of ECC can significantly increase crack saturation within ECC. This results in increased material robustness and ductility. Wang and Li<sup>45</sup> suggested that such flaws have a diameter of approximately 3 to 4 mm ( $0.12$  to  $0.16\ \text{in.}$ ) and be inert to act as voids or flaws within the matrix. EPS beads may be used in future studies to meet these requirements because they showed preliminary success in initiating cracks. This use, however, will not be explored in this article.

In addition to the waste substitutes described previously, virgin components used in both the control ECC and green materials (Table 1) used in this study included Type I ordinary portland cement, virgin silica sand consisting of a gradation curve with 50% particles finer than  $110\ \mu$  ( $0.004\ \text{in.}$ ) and a maximum grain size of  $300\ \mu$  ( $0.012\ \text{in.}$ ) (Fig. 4), ASTM C618 Class F fly ash with particle size of 10 to  $20\ \mu$  ( $0.0004$  to  $0.0008\ \text{in.}$ ) (Fig. 4), ASTM C1017 Type 1 high-range water-reducer, and polyvinyl alcohol (PVA) fibers with a fiber diameter of  $39\ \mu$  ( $0.0016\ \text{in.}$ ) and a length of 8 mm ( $0.3\ \text{in.}$ ). The fiber strength was 1620 MPa (235 ksi), with a tensile elastic modulus of 40 GPa (5800 ksi) (Table 3).

### Infrastructure application integration

Following Fig. 2, preliminary screening was carried out parallel with evaluation of application demands. Minimum required material properties, such as strength, ductility, or permeability, served as goals for iterative tailoring. As a case study, a bridge link slab was chosen for a green ECC structural application. Large-scale implementation of this material design philosophy and the bridge link slab case study are detailed by Lepech and Li.<sup>37</sup>

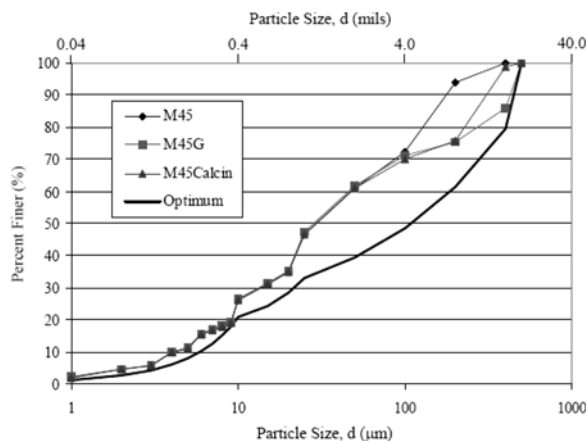


Fig. 5—Grain size distribution of ECC M45, green sand ECC (M45G), bag house ECC (M45Calcin), and optimal Alfred grain size distribution.

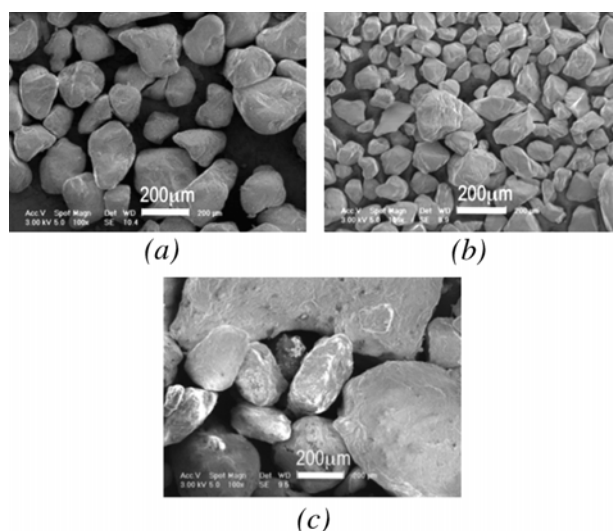


Fig. 6—100 $\times$  magnification of: (a) bag house sand from calcinator; (b) virgin silica sand; and (c) green foundry sand.

To successfully replace bridge expansion joints with a strip of ECC, Kim et al.<sup>35</sup> determined through analytical structural analysis that a minimum of 1.6% tensile ductility was necessary within the ECC link slab. A maximum crack width of 100  $\mu$  (0.004 in.) was required for durability. A minimum compressive strength of 35 MPa (500 psi) was required for traffic. No minimum tensile strength was required. (For this application, tensile strength lower than the concrete in the bridge decks adjacent to the ECC link slab was, in fact, favorable to the designed function of the link slab.) Additionally, the green ECC would have to exhibit flowable fresh properties for on-site casting. These requirements established a target for the materials' tailoring process.

#### Materials tailoring—grain size distribution

ECC M45 mixture proportions (Table 1) had an overall grain size distribution slightly smaller than the optimal Alfred distribution (Fig. 5). This was most prevalent at larger grain sizes. Mixture proportioning using waste foundry sands (bag house sand from calcinator and green foundry sand) focused on reducing separation between the original distribution and the Alfred curve while still meeting micro-mechanical requirements.

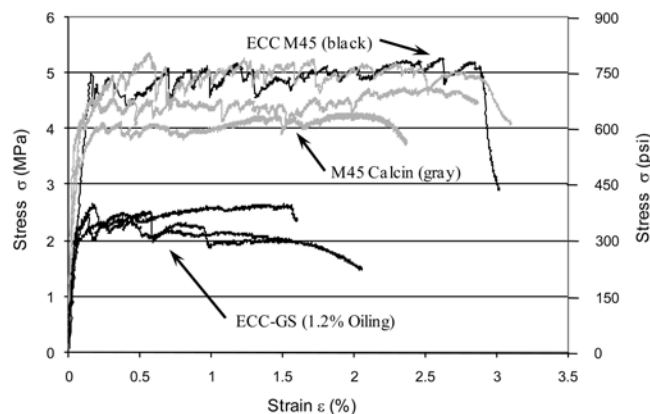


Fig. 7—Typical stress-strain response of ECC M45 and ECC bag house sand from calcinator, and green sand ECC (1.2% fiber oiling content).

Proportioning to match the Alfred curve, the cumulative error between the new mixture designs and the optimal Alfred curve was reduced by roughly 25% over ECC M45, leading to a more flowable fresh state. Mixture proportions are shown in Table 1. Results of flowability tests confirm that new green materials showed improved flowability in the fresh state, as predicted by gradation curves (Table 1). In addition to providing a preliminary tool for evaluation, grain size distribution analysis represents a structured methodology for determining mixture proportions incorporating a number of waste streams (though not attempted in this study). In this case, both foundry sands exhibited improvements over virgin sand for ECC flowability.

#### Materials tailoring—micromechanics

Waste foundry sand from the calcinator bag house was introduced into ECC with little difficulty. With a grain size distribution (Fig. 4) and physical characteristics close to virgin sand (Fig. 6(a) and (b)), virtually no change was observed following complete replacement of virgin sand (Fig. 7). This ECC material exhibited an average compressive strength of 64.8 MPa (9400 psi), an average crack width of 45  $\mu$  (0.002 in.), and a maximum crack width of 75  $\mu$  (0.003 in.). The average tensile strain capacity was 2.6%. Because these met required values, no further tailoring was necessary. This was possibly a unique case in which an industrial waste possessed all of the properties to succeed as a virgin material replacement without re-engineering the material to account for the substitution.

The introduction of most wastes is accompanied by a decrease in performance due to an imbalance of carefully controlled fiber, matrix, and fiber-matrix properties. This was observed with foundry green sand. Following replacement of virgin sand, the average tensile strain capacity dropped to 1.3%, below the 1.6% application minimum (Fig. 7). Average crack widths increased to 76  $\mu$  (0.003 in.), maximum crack widths increased to 112  $\mu$  (0.004 in.), and compressive strength dropped to 60.7 MPa (8800 psi).

This decrease in performance was traced to the metal casting process. Foundry green sand is waste from lost foam metal casting. Within this process, a replica of the desired casting is created through pre-expansion of polystyrene (EPS) into a foam pattern using a pentane blowing agent. This form is then surrounded by compacted sand. Molten metal is poured

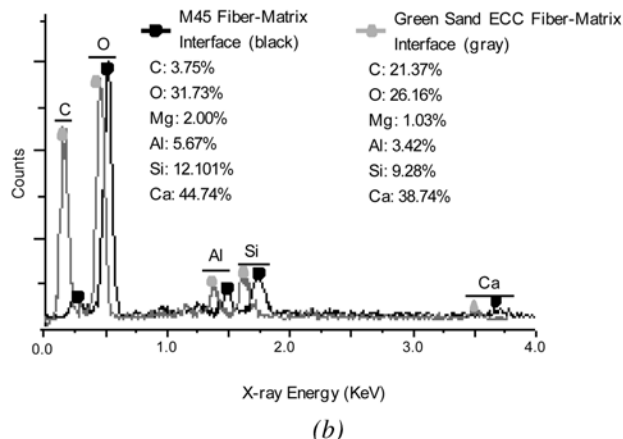
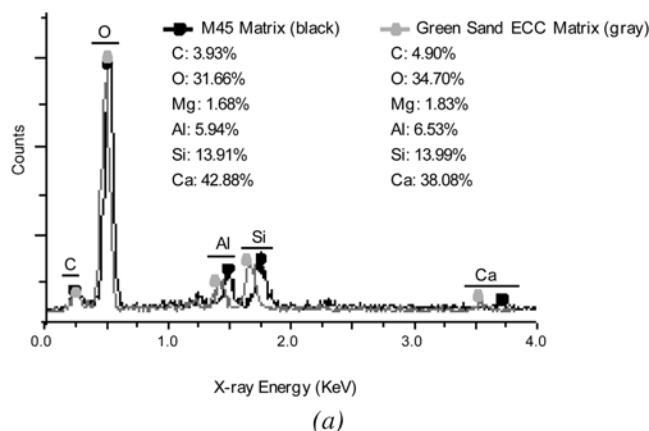


Fig. 8—Chemical composition of: (a) ECC matrix; and (b) ECC fiber-matrix interface for both M45 and green sand ECC (100% green sand replacement).

into the foam mold. As the molten metal melts the foam, it produces a casting identical to the destroyed EPS form.<sup>46,47</sup>

Using clean, virgin sand, the lost foam process produces low-grade finishes that require further machining. To counteract this, treated sands are used for smoother finishes. Treated sand is a combination of dune sand, water, finely ground coal, and clay. Fine coal is used to create a smooth finished surface. As molten metal contacts the treated sand, it burns the coal, creating a thin gas layer between the sand and molten metal. This layer creates a smooth surface. Unburned coal, however, remains on the sand particles after durning and results in a black coloring.

The reduction in strain capacity and increased crack width in ECC containing green sand result from changes within the matrix and fiber-matrix interface due to unburned coal. During mixing, PVA fibers collect coal residue on their surface and exhibit a black coloring that is identical to green sand grains. This residue was verified through XEDS analysis, which found only slightly higher carbon content within green sand matrixes compared with ECC M45 (Fig. 8(a)). This contrasts with the significantly increased carbon content immediately surrounding fibers within the green sand ECC as compared with fiber in ECC M45 matrix (Fig. 8(b)). This points toward a concentration of carbon particles accumulating at the interface of PVA fibers and matrix.

To assess the impact of these changes on strain hardening (characterized by Eq. (3) and (4)), single fiber pullout and matrix fracture toughness tests were conducted. Single fiber pullout tests determine fiber pullout load versus pullout displacement

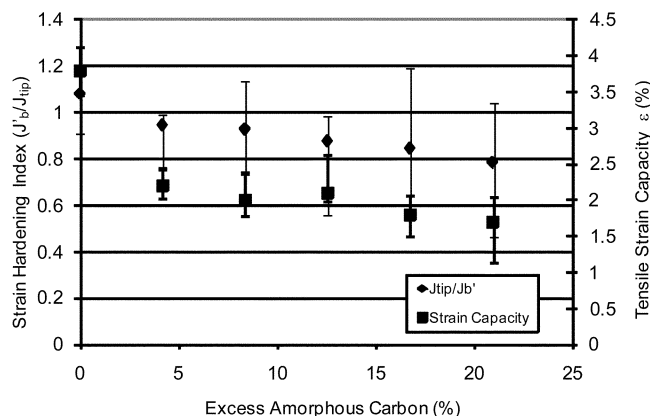


Fig. 9—Strain-hardening index and tensile strain capacity versus excess amorphous carbon content in green sand ECC.

curves ( $p$ - $\delta$ ). This testing follows experimental method procedures detailed by Redon et al.,<sup>48</sup> with ECC material variability summarized by Lepech and Li.<sup>37</sup> The  $p$ - $\delta$  curve is a precursor to the composite  $\sigma$ - $\delta$  relation, used to calculate composite complimentary energy  $J'_b$  (Eq. (3)). This calculation follows the theory described in Li and Leung.<sup>23</sup> The determination of matrix cracking energy of the green sand matrix was performed using notched beam tests. The matrix toughness  $K_m$  was calculated using the appropriate geometric calibration.

The effect of additional carbon on the critical strain-hardening index,  $J'_b/J'_{tip}$ , which must remain above unity for strain-hardening behavior (Eq. (3)), is twofold. First, excess carbon coating the sand particles reduces matrix toughness. The increase in excess amorphous carbon within the ECC matrix from 0 to 9% resulted in a 30% reduction in matrix toughness, from 0.73 to 0.5 MPa m<sup>1/2</sup> (0.66 to 0.45 ksi in.<sup>1/2</sup>). Further addition of excess amorphous carbon resulted in a decrease in matrix toughness to 0.41 MPa m<sup>1/2</sup> (0.37 ksi in.<sup>1/2</sup>). While reducing toughness is desirable to decrease  $J'_{tip}$ , this reduction was coupled with a second phenomenon. A reduction in complimentary energy  $J'_b$  was seen as the carbon particles formed a “sleeve” through which fibers easily slipped out of the matrix and absorbed little energy. Combining these two effects, the strain-hardening ratio ( $J'_b/J'_{tip}$ ) fell below unity. The associated drop in strain capacity is shown in Fig. 9.

Initial development of virgin ECC using PVA fibers showed they performed poorly in cement matrixes due to the hydrophilic nature of PVA.<sup>34</sup> This was due to excessively strong bond that caused fiber rupture during pullout. To reduce bonding, a hydrophobic oiling agent was applied to the fiber surface to reduce rupture failures and increase performance. The application of 1.2% oiling agent (by mass) to the fiber surface was sufficient to lower interfacial bond and yield excellent composite ductility.

However, the combination of 1.2% oiled fibers with the sleeving action provided by excess carbon accumulation results in too little bonding between fiber and matrix. This effect was counteracted by systematically reducing the fiber oiling content to achieve a composites  $\sigma$ - $\delta$  curve similar to M45 ECC. Through systematic reductions in oiling content from 1.2 to 0.3%, an increase in the strain hardening index ( $J'_b/J'_{tip}$ ) above unity was seen (Fig. 10) along with an associated increase in tensile strain capacity, reaching a maximum at 0.3% oiling content (by mass) within a matrix that contained compared with 21% excess amorphous carbon.

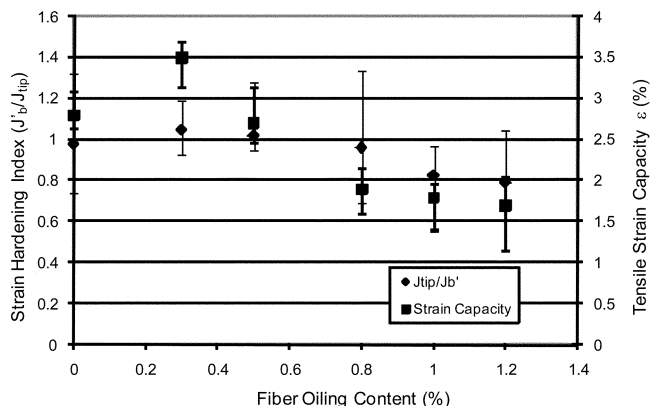


Fig. 10—Strain-hardening index and tensile strain capacity versus fiber oiling content (21% excess amorphous carbon).

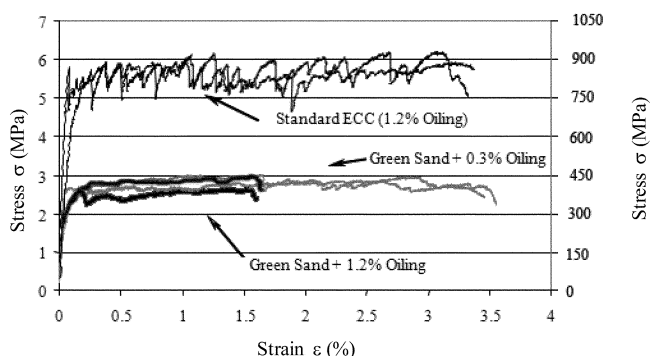


Fig. 11—Typical tensile stress-strain response of green sand ECC with 1.2 and 0.3% fiber oiling content compared with standard ECC M45 with virgin sand.

The combined effect of reducing  $J_{tip}$  and the retention of  $J'_b$  resulted in an increase in the strain-hardening index to approximately 1.05. This resulted in higher ductility in green sand ECC. As shown in Fig. 11, ECC M45 routinely exhibits 3 to 4% tensile strain capacity. After tailoring, green ECC material exhibits a similar tensile strain capacity (Fig. 11). The average compressive strength of green sand ECC was 61.3 MPa (8890 psi), average tensile crack width was 63  $\mu$  (0.0025 in.), and maximum tensile crack width was 85  $\mu$  (0.003 in.). All values meet required link slab application limits. Tensile strength, however, due to the lower matrix fracture toughness, dropped significantly. Had a minimum value for this material property been required, further material design iterations would have been undertaken.

The overall effectiveness of these substitutions was verified by comparing MSI values of ECC M45 with ECC using bag house sand from calcinator and green foundry sand. The calculation of MSI values, detailed in Kendall et al.,<sup>33</sup> relies on life cycle assessment of all material and energy consumption along with water and emission generation associated with raw material extraction and production of ECC and its constituents. Based on this comprehensive environmental assessment, the introduction of foundry sands resulted in the replacement of an additional 22% of virgin ECC materials, whereas solid waste diverted from landfills increased 93%. Additional small reductions in environmental impact were seen in primary energy consumption, carbon dioxide emissions, and criteria pollutant emissions.

## CONCLUSIONS

Materials engineering for increased sustainability is possible through the application of the proposed green materials design framework that combines preliminary analysis techniques, infrastructure application requirements, and micromechanical materials tailoring tools. A large preliminary set of potential substitutes, including industrial wastes, was assessed to gauge their potential within ECC materials. These found that green foundry sand, cement kiln dust, and fly ash served as good potential substitutes. Using an existing micromechanical materials tailoring toolbox, these waste materials were used to replace virgin raw materials within ECC composites.

Following this preliminary assessment, this study focused specifically on the addition of green foundry sand, which was found to reduce green ECC tensile strain capacity by over 50% as compared with virgin materials. This reduction forced ECC material properties below the minimum limits imposed by the bridge deck link slab application identified for green ECC materials. Characterization of the matrix fracture properties and fiber pullout behavior show that, while carbon residue on green foundry sand particles reduces matrix fracture toughness by nearly 40%, a corresponding 80% drop in bridging stress complementary energy eliminates multiple cracking and strain-hardening potential. Re-engineering of the fiber matrix interface to counteract the sleeving action of carbon residue on embedded fibers restored both multiple cracking behavior and strain-hardening potential. Compared with previous versions of ECC material, the introduction of foundry sands resulted in significant environmental improvement in virgin material requirements and landfill waste reduction.

Through the use of the integrated materials design process, in which material properties and processing techniques were tailored to meet a specific structural demand, the links between microstructure and structural performance were further clarified. Although this approach focused primarily on the development of ECC materials, the application of micromechanics to tailor material properties and achieve sustainable infrastructure performance can be broadly applied within the civil engineering and materials design communities.

## ACKNOWLEDGMENTS

The authors would like to thank the U.S. National Science Foundation MUSES Grant (CMS-0223971 and CMS-0329416) for funding this research, and R. Illka with General Motors for providing sample industrial waste streams.

## REFERENCES

1. U.S. Green Building Council, "LEEC-NC v2.0," 2005, pp. 1-81.
2. Green Buildings Council Australia, "Greenstar Office Design," Version 2, 2005.
3. Murakami, S.; Iwamura, K.; Sato, M.; Ikaga, T.; and Endo, J., "Comprehensive Assessment System for Building Environmental Efficiency (CASBEE)," *Proceedings of the Fifth International Conference on Ecobalances*, Nov. 6-8, 2002, pp. 575-578.
4. Siddique, R., "Properties of Concrete Incorporating High Volumes of Class F Fly Ash and Sand Fibers," *Cement and Concrete Research*, V. 34, No. 1, Jan. 2004, pp. 37-42.
5. Su, N., and Miao, B., "A New Method for the Mix Design of Medium Strength Flowing Concrete with Low Cement Content," *Cement and Concrete Composites*, V. 25, No. 2, Feb. 2003, pp. 215-222.
6. Feng, N. Q., and Peng, G. F., "Effect of Mineral Admixtures on Durability of Concrete Structure Subjected to Alkaline Saline Corrosions," *Key Engineering Materials*, V. 302-303, 2006, pp. 68-72.
7. Subramaniam, K. V.; Gromotka, R.; Shah, S. P.; Obla, K.; and Hill, R., "Influence of Ultrafine Fly Ash on the Early Age Response and the Shrinkage Cracking Potential of Concrete," *Journal of Materials in Civil Engineering*, V. 17, No. 1, Jan.-Feb. 2005, pp. 45-53.



8. Jiang, L.; Liu, Z.; and Ye, Y., "Durability of Concrete Incorporating Large Volumes of Low-Quality Fly Ash," *Cement and Concrete Research*, V. 34, No. 8, Aug. 2004, pp. 1467-1469.
9. Wang, F.; Hu, S.; Ding, Q.; and Peng, Y., "Influence of Mineral Admixtures on the Permeability of Lightweight Aggregate Concrete," *Journal of Wuhan University of Technology, Materials Science Edition*, V. 20, No. 2, June 2005, pp. 115-118.
10. Wang, S., and Li, V. C., "Engineered Cementitious Composites with High-Volume Fly Ash," *ACI Materials Journal*, V. 104, No. 3, May-June 2007, pp. 233-241.
11. Manso, J. M.; Gonzalez, J. J.; and Polanco, J. A., "Electric Arc Furnace Slag in Concrete," *Journal of Materials in Civil Engineering*, V. 16, No. 6, Nov.-Dec. 2004, pp. 639-645.
12. Kosmatka, S., and Panarese, W. C., *Design and Control of Concrete Mixes*, 13th edition, Portland Cement Association, Skokie, IL, 1998, p. 69.
13. Michigan Department of Transportation, "2003 Standard Specifications for Construction," Michigan Department of Transportation Publications Office, Lansing, MI, 2003, pp. 689-703.
14. Turatsinze, A.; Bonnet, S.; and Granju, J. L., "Mechanical Characterisation of Cement-Based Mortar Incorporating Rubber Aggregates from Recycled Worn Tires," *Building and Environment*, V. 40, No. 2, Feb. 2005, pp. 221-226.
15. Ferreira, C.; Ribeiro, A.; and Ottosen, L., "Possible Applications for Municipal Solid Waste Fly Ash," *Journal of Hazardous Materials*, B96, 2003, pp. 201-216.
16. Mangialardi, T.; Piga, L.; Schena, G.; and Sirini, P., "Characteristics of MSW Incinerator Ash for Use in Concrete," *Environmental Engineering Science*, V. 15, No. 4, 1998, pp. 291-297.
17. Okpala, D. C., "Some Engineering Properties of Sandcrete Blocks Containing Rice Husk Ash," *Building and Environment*, V. 28, No. 3, 1993, pp. 235-241.
18. Polley, C.; Cramer, S. M.; and de la Cruz, R. V., "Potential Challenges for Using Waste Glass in Portland Cement Concrete," *Journal of Materials in Civil Engineering*, V. 10, No. 4, Nov. 1998, pp. 210-219.
19. Meyer, C., "Concrete as a Green Building Material," *Proceedings of ConMat '05*, Vancouver, BC, Canada, Aug. 22-24, 2005, 380 pp.
20. Keoleian, G. A.; Kendall, A.; Dettling, J. E.; Smith, V. M.; Chandler, R. F.; Lepech, M. D.; and Li, V. C., "Life Cycle Modeling of Concrete Bridge Design: Comparison of ECC Link Slabs and Conventional Steel Expansion Joints," *Journal of Infrastructure Systems*, Mar. 2005, pp. 51-60.
21. Li, V. C., "Reflections on the Research and Development of Engineered Cementitious Composites (ECC)," *Proceedings of the JCI International Workshop on Ductile Fiber Reinforced Cementitious Composites (DFRCC)—Application and Evaluation (DRFCC-2002)*, Takayama, Japan, Oct. 2002, pp. 1-21.
22. Lepech, M. D., and Li, V. C., "Long-Term Durability Performance of Engineered Cementitious Composites," *Journal of Restoration of Buildings and Monuments*, V. 12, No. 2, 2006, pp. 119-132.
23. Li, V. C.; Leung, C. K. Y., "Theory of Steady State and Multiple Cracking of Random Discontinuous Fiber Reinforced Brittle Matrix Composites," *Journal of Engineering Mechanics*, ASCE, V. 118, No. 11, 1992, pp. 2246-2264.
24. Li, V. C.; Wang, S.; and Wu, C., "Tensile Strain-Hardening Behavior of PVA-ECC," *ACI Materials Journal*, V. 98, No. 6, Nov.-Dec. 2001, pp. 483-492.
25. Lepech, M., and Li, V. C., "Water Permeability of Cracked Cementitious Composites," Paper 4539 of Compendium of Papers, ICF 11, Turin, Italy, Mar. 2005. (CD-ROM)
26. PCA, "Technical Brief: Green in Practice 102—Concrete, Cement, and CO<sub>2</sub>," Portland Cement Association, Skokie, IL, <http://www.concretethinker.com/Papers.aspx?DocId=312> (accessed Aug. 2006).
27. Hendricks, C. A.; Worrell, E.; Price, L.; Martin, N.; Ozawa Meida, L.; de Jager, D.; and Reimer, P., "Emission Reduction of Greenhouse Gases from the Cement Industry," *Proceedings of the Fourth International Conference on Greenhouse Gas Control Technologies*, Interlaken, 1998, pp. 939-944.
28. Worrell, E.; Price, L.; Martin, N.; Hendricks, C.; and Ozawa Meida, L., "Carbon Dioxide Emissions from the Global Cement Industry," *Annual Reviews of Energy and the Environment*, V. 26, pp. 303-329.
29. WBCSD, "Toward a Sustainable Cement Industry," draft report for the World Business Council on Sustainable Development, Battelle Memorial Institute, <http://www.wbcd.org/DocRoot/C4uPdILJR31Jn8CO1q3w/batelle-full.pdf> (accessed 2002).
30. U.S. EPA, "CFR Part 63 National Emissions Standards for Hazardous Air Pollutants for Source Categories; Portland Cement Manufacturing Industry; Final Rule," U.S. Environmental Protection Agency, 2003, <http://www.epa.gov/ttn/atw/pcem/fr14jn99.html>.
31. U.S. EPA, "Sources of Dioxin-like Compounds in the United States," Draft Exposure and Human Health Assessment of 2,3,7,8-tetrachlorodibenzo-p-dioxin (TCDD) and Related Compounds, EPA/600/P-00/001 Bb. United States Environmental Protection Agency, 2000, <http://cfpub.epa.gov/ncea/cfm/part1and2.cfm>.
32. Keoleian, G.; Kendall, A.; Lepech, M.; and Li, V. C., "Guiding the Design and Application of New Materials for Enhancing Sustainability Performance: Framework and Infrastructure Application," *Proceedings, Materials Research Society*, V. 895, 2006.
33. Kendall, A.; Keoleian, G. A.; and Lepech, M., "Material Design for Sustainability through Life Cycle Modeling of Engineered Cementitious Composites," *Materials and Structures*, V. 41, No. 6, July 2008, pp. 1117-1131.
34. Li, V. C.; Wang, S.; and Wu, C., "Tensile Strain-Hardening Behavior of PVA-ECC," *ACI Materials Journal*, V. 98, No. 6, Nov.-Dec. 2001, pp. 483-492.
35. Kim, Y. Y.; Fischer, G.; and Li, V. C., "Performance of Bridge Deck Link Slabs Designed with Ductile ECC," *ACI Structural Journal*, V. 101, No. 6, Nov.-Dec. 2004, pp. 792-801.
36. Fischer, G.; Wang, S.; and Li, V. C., "Design of Engineered Cementitious Composites for Processing and Workability Requirements," *Seventh International Symposium on Brittle Matrix Composites*, Warsaw, Poland, 2003, pp. 29-36.
37. Lepech, M. D., and Li, V. C., "Large-Scale Processing of Engineered Cementitious Composites," *ACI Materials Journal*, V. 105, No. 4, July-Aug. 2008, pp. 358-366.
38. Funk, J. E., and Dinger, D. R., "Particle Packing, Part VI—Applications of Particle Size Distribution Concepts," *Interceram*, V. 43, No. 5, 1994, pp. 350-353.
39. Kong, J. H.; Bike, S.; and Li, V. C., "Development of a Self-Consolidating Engineered Cementitious Composite Employing Electrosteric Dispersion/Stabilization," *Journal of Cement and Concrete Composites*, V. 25, No. 3, 2003, pp. 301-309.
40. Marshall, D. B., and Cox, B. N., "A J-Integral Method for Calculating Steady-State Matrix Cracking Stresses in Composites," *Mechanics of Materials*, No. 8, 1988 pp. 127-133.
41. Li, V. C., and Leung, C. K. Y., "Theory of Steady State and Multiple Cracking of Random Discontinuous Fiber Reinforced Brittle Matrix Composites," *Journal of Engineering Mechanics*, ASCE, V. 118, No. 11, 1992, pp. 2246-2264.
42. Lin, Z.; Kanda, T.; and Li, V. C., "On Interface Property Characterization and Performance of Fiber Reinforced Cementitious Composites," *Journal of Concrete Science and Engineering*, RILEM, V. 1, 1999, pp. 173-184.
43. Kim, Y. Y.; Kim, J. S.; Ha, G. J.; and Kim, J. K., "Influence of ECC Ductility on the Diagonal Tension Behavior (Shear Capacity) of Infill Panels," *Proceedings of the International RILEM Workshop on High Performance Fiber Reinforced Cementitious Composites in Structural Applications*, Honolulu, HI, May 23-26, 2005, pp. 403-410.
44. Illka, R., "Saginaw Metal Casting Operations 2003 Annual Waste Characterization for Lost Foam and Green Sand Casting Operations," General Motors Corp., Saginaw, MI, 2003, 1 p.
45. Wang, S., and Li, V. C., "Tailoring of Pre-existing Flaws in ECC Matrix for Saturated Strain Hardening," *Proceedings of FRAMCOS-5*, Vail, CO, Apr. 2004, pp. 1005-1012.
46. Naik, T. R.; Patel, V. M.; Parikh, D. M.; and Tharaniyil, M. P., "Utilization of Used Foundry Sand in Concrete," *Journal of Materials in Civil Engineering*, V. 6, No. 2, 1992, pp. 254-263.
47. Schey, J. A., *Introduction to Manufacturing Processes*, McGraw-Hill, Boston, MA, 2000, p. 168.
48. Redon, C.; Li, V. C.; Wu, C.; Hoshiro, H.; Saito, T.; and Ogawa, A., "Measuring and Modifying Interface Properties of PVA Fibers in ECC Matrix," *Journal of Materials in Civil Engineering*, ASCE, V. 13, No. 6, Nov.-Dec. 2001, pp. 399-406.
49. Realf, M. J.; Ammons, J. C.; and Newton, D., "Carpet Recycling: Determining the Reverse Production System Design," *Polymer-Plastics Technology and Engineering*, V. 38, No. 3, 1999, pp. 547-567.
50. Zhu, W. H.; Tobias, B. C.; Coutts, R. S. P.; and Lanfors, G., "Air-Cured Banana Fibre-Reinforced Cement Composites," *Cement and Concrete Composites*, V. 16, No. 1, 1994, pp. 3-8.